Journal of Colloid and Interface Science 330 (2009) 29–37

Contents lists available at ScienceDirect

Journal of Colloid and Interface Science

www.elsevier.com/locate/jcis

Removal of Cu^{2+} from aqueous solution by chitosan-coated magnetic nanoparticles modified with α-ketoglutaric acid

Yu-Ting Zhou [a], Hua-Li Nie [a], Christopher Branford-White [b], Zhi-Yan He [a], Li-Min Zhu [a,*]

[a] College of Chemistry, Chemical Engineering and Biotechnology, Donghua University, Shanghai 201620, China
[b] Institute for Health Research and Policy, London Metropolitan University, 166–220 Holloway Road, London, UK

ARTICLE INFO

Article history:
Received 25 June 2008
Accepted 10 October 2008
Available online 17 October 2008

Keywords:
Nanoadsorbents
α-Ketoglutaric acid (α-KA)
Adsorption isotherm
Desorption
Cu^{2+} removal

ABSTRACT

Chitosan-coated magnetic nanoparticles (CCMNPs), modified with a biodegradable and eco-friendly biologic reagent, α-ketoglutaric acid (α-KA), was used as a magnetic nanoadsorbent to remove toxic Cu^{2+} ions from aqueous solution. The prepared magnetic nanoadsorbents were characterized by FTIR, TEM, VSM, XRD, and EDS. Factors influencing the adsorption of Cu^{2+}, e.g., initial metal concentration, initial pH, contact time and adsorbent concentration were investigated. TEM images show that the dimension of multidispersed circular particles is about 30 nm and no marked aggregation occurs. VSM patterns indicate superparamagnetic properties of magnetic nanoadsorbents. EDS pictures confirm the presence of the Cu^{2+} on the surface of magnetic nanoadsorbents. Equilibrium studies show that Cu^{2+} adsorption data follow Langmuir model. The maximum adsorption capacity (q_{max}) for Cu^{2+} ions was estimated to be 96.15 mg/g, which was higher than that of pure CCMNPs. The desorption data show no significant desorption hysteresis occurred. In addition, the high stability and recovery capacity of the chitosan-coated magnetic nanoparticles modified with α-ketoglutaric acid (α-KA-CCMNPs) suggest that these novel magnetic nanoadsorbents have potential applications for removing Cu^{2+} from wastewater.

1. Introduction

The environment and all the life forms on earth face a very serious threat from the heavy metal pollution due to rapid industrialization and the growth in the world population [1]. At least 20 metals are classified as toxic and half of these are emitted into the environment in quantities that pose risk to human health [2]. Copper (Cu^{2+}), an abundant and naturally occurring element present in municipal wastewaters, is one of such heavy metals harmful to human health. If copper is ingested excessively in the human diet, it may result in vomit, cramps, convulsion, and even death. On the other hand, the lack of Cu^{2+} in animal diet may lead to anemia, diarrhea, and nervous disturbances [3]. Moreover, enzymes, whose activities depend on sulhydryl and amino groups [4], are strongly inhibited by Cu^{2+} ions which have high affinity for N and S containing donor ligands [5]. Therefore, it is of great practical interest to explore ways to effectively remove these heavy metal ions from the wastewaters before their discharge, and to possibly separate them for recovery and re-use.

Numerous technologies have been developed for the removal of Cu^{2+} from industrial wastewater, such as chemical precipitation, ion exchange, liquid–liquid extraction and resins, cementation, electrodialysis, and biosorption [6,7]. Each method has been found to be limited for the cost, complexity and efficiency, as well as secondary wastes. For example, the electrolysis processes often take higher operational costs, and the chemical precipitation may generate secondary wastes [8,9]. Another example is that, remediation technologies of Cr(VI) from wastewater have been carried out from many years, but successive applications are limited [10]. Thus, among these various processes, biosorption, which uses cheap and non-pollutant adsorption materials, may be an alternative wastewater technology, in which technological, environmental and economic constraints are taken into consideration. And this method can avoid the generation of secondary waste, and the adsorption materials employed in this method can be recycled and used easily on an industrial scale.

The search for new adsorbents is an important factor in improving analytical sensitivity and precision in biosorption techniques [11]. However, traditional adsorbents show poor recovery of the target metal ions from large volumes of solution due to low binding capacity, diffusion limitations and the lack of active surface sites. Hence, it would be of great interest to develop a novel adsorbent with a large adsorptive surface area, low diffusion resistance, high adsorption capacity and fast separation for large volumes of solution [11]. Recently, magnetic separation techniques have attracted lots of attentions due to the specific char-

* Corresponding author. Fax: +86 21 67792655.
E-mail address: lzhu@dhu.edu.cn (L.-M. Zhu).

0021-9797/$ – see front matter
doi:10.1016/j.jcis.2008.10.026

acteristics. Magnetic separation may become one of the promising ways for environment purification technique because it produces no contaminants, and has the capability of treating large amount of wastewater within a short time [12]. Moreover, this approach is particularly adapted when the condition of separation is complex, i.e., when polluted water contains solid residues which exclude their treatment in column with regards to the risks of filling [12]. Because these magnetic particles are superparamagnetic, that is, they do not become permanently magnetized without the external magnetic field. The superparamagnetic particles adsorbing target metal ions can be removed very quickly from a matrix using a magnetic field, and be reused without losing active sites. Therefore, magnetic separation has been gradually employed as a recovery and pollution-control process for many environmental and industrial processes. Nanometer-sized materials have also attracted substantial interest in the scientific community because of their special properties [13]. The relatively large surface area and highly active surface sites of nanoparticles enable them to possess higher adsorption capacity compared with the previous adsorbents. Thus, an adsorbent combining with magnetic separation techniques and nanometer-sized materials, which can be easily recovered or manipulated with an external magnetic field, can be used as an alternative large scale wastewater treatment procedure.

Numerous types of magnetic nanoparticles for heavy metals removal could be tailored by using functionalized natural or synthetic polymers to impart surface reactivity [1]. Hu et al. [14] employed δ-FeOOH-coated maghemite as adsorption material for the removal and recovery of Cr(VI) from wastewater, and Shashwat et al. [1] utilized gum Arabic modified magnetic to do that. And Kochen et al. [15] used magnetic polymer resin for the removal of actinides and other heavy metals from contaminated water. The removal of nickel ions from aqueous solution by magnetic alginate microcapsules was reported by Ngomsik et al. [16]. And Chang et al. [17] reported chitosan-bound Fe_3O_4 magnetic nanoparticles for removal of Cu^{2+} ions. Although there are reports on the effectiveness of the inorganic-coated or organic-coated magnetic particles on the removal of heavy metals [18,19], the chemical modification of these coated magnetic adsorbents and the potential effectiveness of these coated magnetic adsorbents modified with biologic reagent have not been discussed.

In this study, a novel magnetic nanoadsorbent for the removal of Cu^{2+} was firstly developed by the surface modification of chitosan-coated magnetic nanoparticles (CCMNPs) with α-ketoglutaric acid (α-KA), which is a natural, inexpensive, harmless and environmental friendly biologic reagent containing active functional groups like carboxyl groups. These magnetic nanoadsorbents were carefully characterized before investigating their adsorption capacity of Cu^{2+} through adsorption isotherms. Their adsorption capacity was demonstrated using Cu^{2+} ions, and compared with that of unmodified CCMNPs. The best adsorption conditions for Cu^{2+} from aqueous solution were determined at various initial ion concentration, initial pH, contact time and adsorbent concentration. The uptake stability of Cu^{2+} from aqueous solution and the regeneration of magnetic nanoadsorbents were carried out by adsorption and desorption process.

2. Materials and methods

2.1. Materials

$CuSO_4 \cdot 5H_2O$ ($M_w = 249.68$ g/mol, purity >99%) from Sinopharm Chemical Reagent Co., Ltd., Shanghai, China, were used as copper source. α-KA (99%), chitosan ($M_w = 6 \times 10^5$ with 80% deacetylation degree), ferric chloride 6-hydrate, ferrous chloride and sodium hydroxide (29.6%) were obtained from Sinopharm Chemical Reagent Co., Ltd., Shanghai, China. Highly pure deionized water (Shanghai Jingke Industrial Co., Ltd., SZ-93) obtained from a Labconco system (Shanghai Jingke Industrial Co., Ltd., China) was used throughout this work, and was used for the preparation of all of the solutions. All other chemicals were the analytic grade reagents commercially available, and used without further purification.

2.2. Preparation of maghemite nanoparticles

The maghemite nanoparticles were prepared by the existing method from Kang et al. [20]. Firstly, 6.7 g $FeCl_3 \cdot 6H_2O$ and 3.06 g $FeCl_2$ were dissolved in the 200 ml of deionized water under mechanical stirring, while the molar ratio of the Fe^{3+}/Fe^{2+} was fixed to 2:1. Then NaOH (5 M) solution was added dropwise into the above mixture with mechanical stirring until pH reached about 10. After an initial yellow solution, a brown precipitate was immediately formed. The brown precipitate was then heated at 80 °C for 30 min under vigorous stirring. Subsequently, the brown precipitate was isolated by an external magnetic field of 3000 G with the supernate decanted. To get the maghemite (γ-Fe_2O_3), freeze-dried brown precipitates were dispersed in 99% octyl ether. And the mixture was then heated to 250 °C under an air atmosphere, and maintained at this temperature for 2 h. The γ-Fe_2O_3 was collected via an external magnetic field after adding ethanol. To obtain the pure products, synthesized materials were rinsed with deionized water three times, and finally stored in 5 M NaOH solution for further use.

2.3. Preparation of CCMNPs

For coating magnetic nanoparticles with chitosan, 10 ml the above obtained maghemite solution and 1 ml Span-80 were dispersed in 50 ml chitosan solution (16%) which was prepared using 0.8 g chitosan dissolved in 25 wt% acetum solution under vigorous stirring of 2000 rpm. The reaction mixture was then sonicated in an ultrasonic cleaner (Shanghai Kudos Ultrasonic Instrument Co., Ltd., SK5200H) for 30 min. The coating process was carried out at 50 °C. The CCMNPs were recovered from the reaction mixture by placing the bottle on a permanent magnet with a surface magnetization of 3000 G. The prepared CCMNPs settled within 1–3 min, and then were washed with deionized water three times.

2.4. Surface modification of CCMNPs with α-KA

The α-KA-CCMNPs were produced according to the existing chemical method [21]. With mechanical stirring, 0.25 g α-KA was added to 5 ml acetic acid buffer (pH 5.6) which contained 100 mg CCMNPs. The pH of this mixture was adjusted to 4.5–5.0 using sodium hydroxide solution. Afterwards, sodium borohydride was added to the stirred mixture at 35 °C. The pH of the mixture solution was adjusted to 6.5–7.0 using hydrochloric acid solution, and the reaction was further stirred for 24 h. The reaction was terminated by 95% alcohol. The synthesized α-KA-CCMNPs were isolated, washed three to four times with ethanol and diethyl either, respectively. Subsequently, the products were dried in an oven. Finally, 53 mg α-KA-CCMNPs were obtained and characterized before their application.

2.5. Characterizations of the α-KA-CCMNPs

The dimension and morphology of CCMNPs and γ-Fe_2O_3 were observed by transmission electron microscopy (TEM) (Hitachi, H-800). The elemental information and structure of synthesized α-KA-CCMNPs were determined by an X-ray diffractometer (XRD) (Rigaku, D/max-2550PC) at ambient temperature. The instrument was equipped with a copper anode generating Cu$K\alpha$ radiation

($\lambda = 1.54056$ Å). Magnetization measurements were preformed with VSM (Princeton Applied Research, model-155) at room temperature. Hysteresis measurements conducted at 300 K on freeze-dried samples with applied magnetic field up to 1 T. The α-KA-CCMNPs were also characterized by using Fourier-transform infrared spectroscopy (FTIR) (Nicolet, Nexus-670). A background spectrum was measured on pure KBr. The adsorption capacity of α-KA-CCMNPs was identified by UV–visible spectrophotometry (Unico (Shanghai) Instrument Co., Ltd., UV-2102 PC). The presence of Cu^{2+} ions on the surface of α-KA-CCMNPs is documented by energy dispersive X-ray spectrometer (EDS). Metal-loaded and metal-free (control) α-KA-CCMNPs were treated with glutaraldehyde for 1 h, and were dehydrated by acetone (50–100%) for 30 min. The pre-treated samples were coated with Au via vapor deposition prior to being introduced to EDS (Oxford, IE 300 X) for analysis.

2.6. Batch adsorption studies

Adsorption of Cu^{2+} by synthetic α-KA-CCMNPs was investigated by batch experiments. In the first instance, the effect of contact time was studied following the batch technique. In each experiment, 50 mg of α-KA-CCMNP was suspended in a 10 ml of 200 ppm concentration of Cu^{2+} solution taken in a 100 ml flask, and shaken at 100 rpm in a shaker bath at $22 \pm 2\,^{\circ}C$ for an appropriate time to ensure the adsorption process to reach equilibrium. In order to mix the Cu^{2+} solution and α-KA-CCMNP completely, and not bring other problems such as adsorbents bonding to the wall of flask, the prepared $CuSO_4$ solution was injected into the flask by micropipette. Moreover, before batch experiment the pH of the Cu^{2+} solution was adjusted by standard acid 1 M HCl and base 1 M NaOH solutions. Subsequently, the α-KA-CCMNPs as magnetic nanoadsorbents were separated via an external magnetic field (3000 G), and washed using deionized water repeatedly. The filtrate was collected for Cu^{2+} analysis. And the concentration of residual $CuSO_4$ solution was analyzed spectrophotometrically at 740 nm using Na_2EDTA reagent as a complexing agent. It has to be noted that during experimentation, in all samples no release of magnetic nanoparticles was observed, and there is no control over the pH of the solution. Similar batch experiments were performed to study the influence of pH (range: 2.0–8.0), initial Cu^{2+} concentration (range: 40–800 ppm), and magnetic nanoadsorbent dose (range: 1–12 g/L).

Isotherm experiments were performed with different initial Cu^{2+} concentration solution (40–800 ppm, according to the previous reports [22–24]) by adding a constant dose of α-KA-CCMNPs of 5 g/L. Among them the Tris–HCl buffer was used, and metal solution was maintained at desired pH values of 6.0 to achieve the optimum adsorption environment. To compare with CCMNPs, a series of 10 ml of Cu^{2+} solution in the same concentration range of 40–800 ppm was prepared, and brought into contact with the same amount of 50 mg CCMNPs. For these experiments, the flasks were shaken at a speed of 100 rpm and room temperature ($22 \pm 2\,^{\circ}C$) for the required contact time. The initial pH of the solution was adjusted to 6.0 as optimized. The adsorbed amount of Cu^{2+} ion per unit weight of α-KA-CCMNPs at time t, $q(t)$ (mg/L) was calculated from the mass balance equation as

$$q(t) = \frac{(C_0 - C_t)V}{m}, \tag{1}$$

where C_0 and C_t (mg/L) are the initial Cu^{2+} ion concentration and the Cu^{2+} ion concentrations at any time t, respectively; V the volume of the Cu^{2+} ion solution; and m is the weight of α-KA-CCMNP.

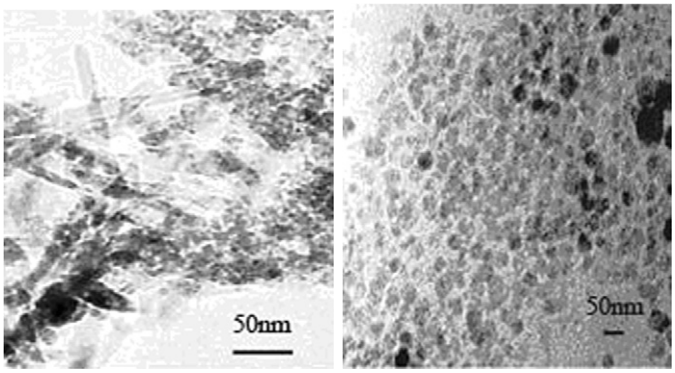

(a) (b)

Fig. 1. TEM images of (a) γ-Fe_2O_3 and (b) CCMNPs.

The removal efficiency (E) of adsorbent on Cu^{2+} was measured as follows:

$$E(\%) = \frac{C_0 - C_f}{C_0} \times 100, \tag{2}$$

where C_0 and C_f are the initial and final equilibrium concentration of Cu^{2+} (mg/L) in aqueous solution, respectively.

All experiments were performed three times, and the averaged values were taken and were reported here. The maximum deviation observed was less than 5%.

2.7. Desorption and regenerated studies

Desorption studies were examined by mixing 50 mg Cu-loaded chitosan-coated magnetic nanoparticles modified with α-ketoglutaric acid (Cu-α-KA-CCMNPs) with 10 ml of 0.1 and 0.025 M Na_2EDTA, 0.1 and 0.025 M acetum solution, 0.1 and 0.025 M HCl, and 0.1 and 0.025 M citric acid, respectively. To study the regeneration of α-KA-CCMNPs, seven consecutive cycles of adsorption–desorption process were carried out. For each cycle, 10 ml of 200 ppm Cu^{2+} solution was adsorbed by 50 mg α-KA-CCMNPs for 3 h, and then desorbed with 10 ml of 0.01 M Na_2EDTA solution, which was often chosen as an eluent for the adsorbents in the literature [25]. After each cycle of adsorption–desorption process, α-KA-CCMNPs were washed thoroughly with deionized water to neutralize, and recondition the samples for adsorption in the succeeding seven cycles. After adsorption or desorption had reached equilibrium, α-KA-CCMNPs were separated via an external magnetic field, and the supernate was collected for metal concentration measurements. The optimum pH, initial metal concentration, adsorbent dosage and contact time from above experiments were applied for adsorption–desorption processes.

3. Results and discussion

3.1. Characterization of α-KA-CCMNPs

The TEM images of γ-Fe_2O_3 and CCMNPs are shown in Figs. 1a and 1b. The TEM pattern of γ-Fe_2O_3 (Fig. 1a) shows monodisperse rodlike and rhombohedral shape with the particle sizes of 110 and 10 nm, respectively, while the TEM picture of the CCMNPs (Fig. 1b) shows discrete spherical shape. It was reported that the shapes of the Fe_2O_3 products are rodlike to spherical, and the particle size of the sample had been clearly changed after modification by the surfactants [26]. Fig. 1b also reveals that the CCMNPs synthesized in this study are multidispersed with a mean diameter of around 30 nm, and no marked aggregation occurs. It is known that the small sized nanoparticles are in favor of their suspension in water [27]. In comparison with these two TEM images,

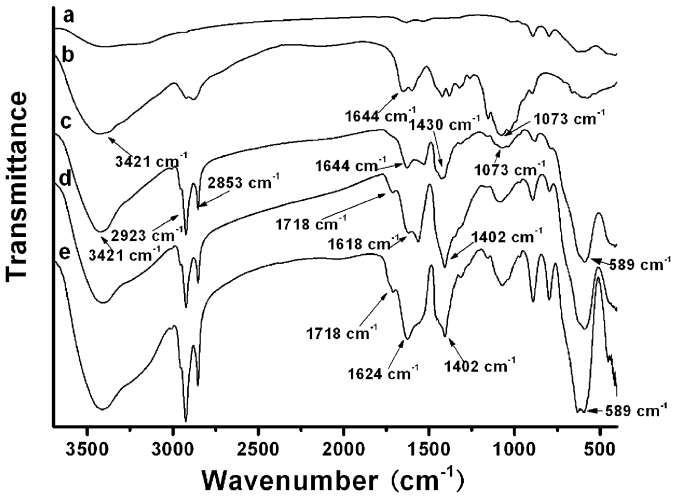

Fig. 2. FTIR spectra for (a) γ-Fe_2O_3, (b) chitosan polymer, (c) CCMNPs, (d) α-KA-CCMNPs and (e) α-KA-CCMNPs (after 100 mmol/L Na_2EDTA desorption).

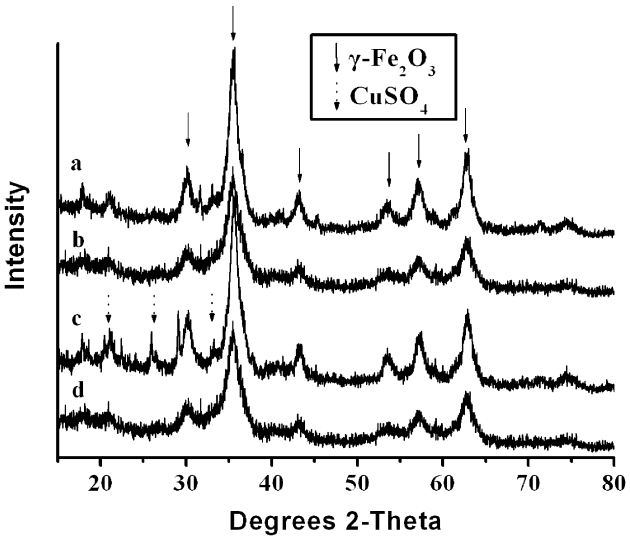

Fig. 3. XRD patterns of (a) CCMNPs, (b) α-KA-CCMNPs, (c) Cu-α-KA-CCMNPs and (d) α-KA-CCMNPs (after 100 mmol/L Na_2EDTA desorption).

it was difficult to find evidence in the TEM photos of the core/shell structure of the CCMNPs directly. However, it can be clearly seen that the chitosan coating process significantly altered the γ-Fe_2O_3 morphology. These findings show that the γ-Fe_2O_3 was coated by the chitosan, and the prepared CCMNPs exhibited good distribution. Moreover, it is notable that no free γ-Fe_2O_3 particles are discernible in the TEM pattern of the CCMNPs.

To confirm the existence of the surface coating, the magnetic nanoparticles before and after the chitosan coating procedure were investigated using the FTIR technique. Fig. 2 exhibits the FTIR spectra of γ-Fe_2O_3 (a), chitosan polymer (b) and CCMNPs (c), respectively. By comparison of the FTIR patterns (Figs. 2a and 2c), the presence of the chitosan coating changed the FTIR pattern of γ-Fe_2O_3 (Fig. 2a) significantly. As seen in Fig. 2c, the peak at 3421 cm^{-1} corresponds to stretching vibration of hydroxyl. And the C–H stretching vibration of the polymer backbone is manifested through strong peaks at 2923 and 2853 cm^{-1}. Besides, the stretch vibration of C–O is found at 1073 and 1031 cm^{-1}. They are also present in the case of the chitosan polymer with similar intensities. The adsorption bands around 3421 and 1644 cm^{-1} observed in two spectra are attributed to the deformation vibration of N–H in primary amine ($-NH_2$). The characteristic adsorption peak of magnetic fluid also appears at round 589 cm^{-1}. This peak indicates the presence of γ-Fe_2O_3 as a result of the successful coating procedure. The other bands are similar for both chitosan polymer and CCMNPs. The findings also imply that the magnetic nanoparticles are coated by the chitosan polymer, and a chemical bond does not form between the chitosan polymer and the magnetic nanoparticles. This may be another reason for the presence of the chitosan polymer of the CCMNPs.

In order to ensure that the α-KA was modified on the surface of CCMNPs, FTIR spectra of CCMNPs treated by this compound was recorded. Figs. 2c and 2d show the FTIR spectra of CCMNPs and α-KA-CCMNPs, respectively. In a comparison of the two FTIR spectra (Figs. 2c and 2d), it can be clearly seen that the chemical modification significantly altered the FTIR pattern of CCMNPs. In the spectrum of α-KA-CCMNPs (Fig. 2d), the characteristic absorption band around 1644 cm^{-1} attributed to the vibration of N–H in primary amine ($-NH_2$) is not observed, while a new sharp peak at 1618 cm^{-1} assigned to the vibration of N–H in secondary amine (–NH) is observed. Furthermore, only the absorption bands at 1718 and 1402 cm^{-1} can be observed in Fig. 2d, but not present in Fig. 2c. The absorbance band at 1402 cm^{-1} is the C–H stretch vibration from R–CH_2–COOH, and the absorbance band at 1718 cm^{-1} shows the presence of the carbonyl groups. The other bands are similar for both CCMNPs and α-KA-CCMNPs. It has to be noted that washing α-KA-CCMNPs many times with ethanol and diethyl ether and then ultrasonic dispersing made sure that the free modifier was removed completely. Thus, these results confirm an interaction of the modifier with CCMNPs. Moreover, the XRD patterns of α-KA-CCMNPs before and after the modification process also illustrated the existence of the α-KA. It can be implied from Figs. 3a and 3b that both the CCMNPs crystal and the mass of the α-KA do not change the patterns of XRD significantly. The γ-Fe_2O_3 is identified from the XRD patterns by the peak positions at 30.24 (220), 35.63 (311), 43.28 (400), 53.73 (422), 57.27 (511) and 62.92 (440), which are in agreement with γ-Fe_2O_3 standard data. By further comparing Fig. 3a with Fig. 3b, the XRD diffraction peaks of γ-Fe_2O_3 (Fig. 3b) become lower and broader, suppressing the appearance of the XRD peaks of γ-Fe_2O_3. This finding indicates that the α-KA modifies uniformly CCMNPs. This is in agreement with reported data on other magnetite/polymer systems, and is mainly attributed to the decrease in the crystallite size [28].

In order to test if the obtained α-KA-CCMNPs could be used as a magnetic nanoadsorbent in the magnetic separation procedures, magnetization measurements were performed with VSM. It is known that particles with the size less than 40 nm offer a large surface area and superparamagnetic properties [29]. Fig. 4 gives typical magnetization loops for the CCMNPs, α-KA-CCMNPs, and the Cu-α-KA-CCMNPs, where no reduced remanence and coercivity are observed. Because of no remanence and coercivity, it is suggested that such α-KA-CCMNPs, as magnetic nanoadsorbents, are superparamagnetic. The saturation magnetizations of the CCMNPs, the α-KA-CCMNPs and the Cu-α-KA-CCMNPs are 40, 33.5 and 30.5 emu/g, respectively, which are higher than or comparable to other resins produced by dispersion-polymerization or suspension-polymerization [30–33]. These large saturation magnetization and superparamagnetic properties make α-KA-CCMNPs very susceptible to the external magnetic field, and possibly reusable without aggregation after removing the external magnetic field. Moreover, the superparamagnetic properties have no significant change when CCMNPs were modified with α-KA, and the Cu-α-KA-CCMNPs were formed.

In order to probe Cu^{2+} ions adsorbed onto α-KA-CCMNPs, α-KA-CCMNPs before and after adsorption were collected for the EDS studies. The EDS spectra and analyses of α-KA-CCMNPs and Cu-α-KA-CCMNPs are depicted in Figs. 5a and 5b. Comparing Fig. 5a with Fig. 5b, it is found that the EDS analysis give a direct

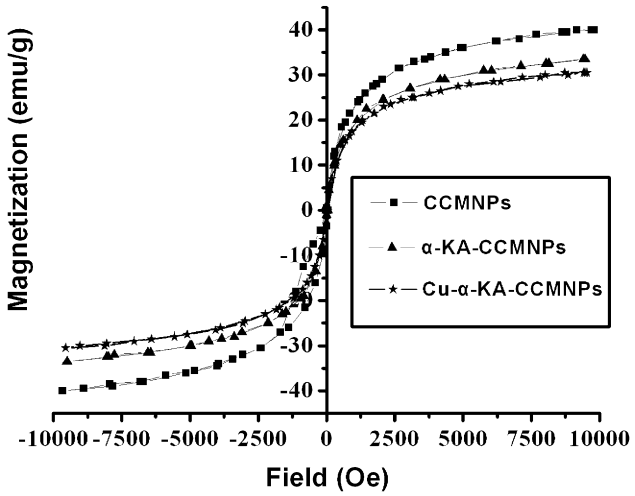

Fig. 4. VSM curves of the CCMNPs, the α-KA-CCMNPs and the Cu-α-KA-CCMNPs.

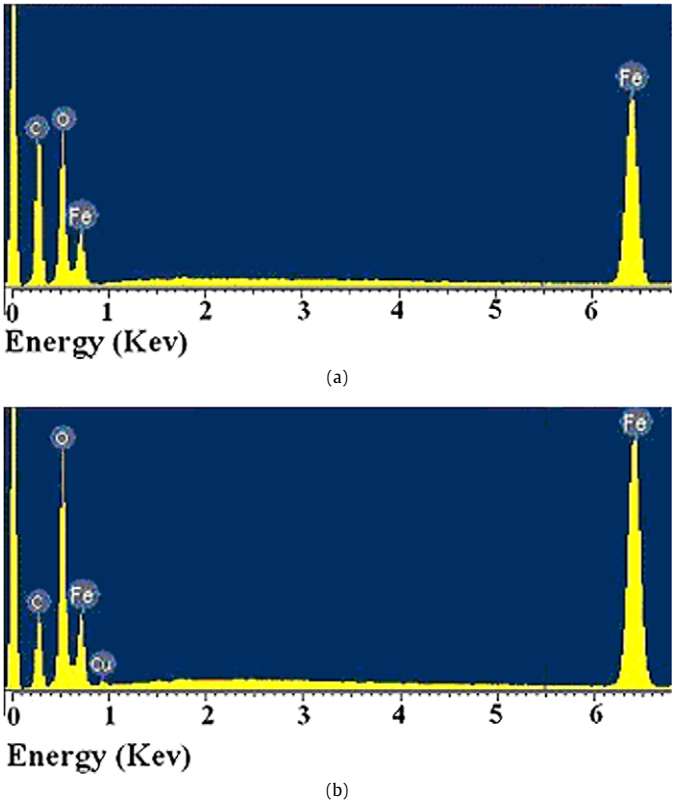

Fig. 5. EDS analysis of (a) α-KA-CCMNPs (before adsorption) and (b) Cu-α-KA-CCMNPs.

detection of the presence of metal adsorbates on α-KA-CCMNPs. Note that most adsorption studies determined metal sorption by measuring the residual metal concentrations in the supernatant, and did not directly prove the presence of the metals on the adsorbents. Moreover, the composition of α-KA-CCMNPs obtained from the EDS analysis was further investigated. The elements identified are iron and oxygen. Namely, Fe and O are the major constituents in α-KA-CCMNPs, and no other elements are detected. Through calculation of the atomic percentages, the atom ratio of Fe and O is about 2:3, which indicates that the magnetic part of α-KA-CCMNPs is the pure γ-Fe_2O_3. This is consistent with the results deduced from XRD inspection.

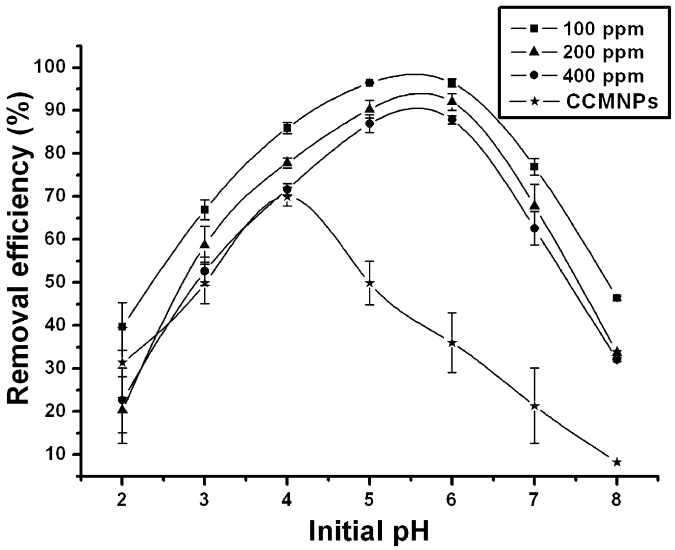

Fig. 6. Effect of initial pH and initial concentration on the removal of Cu^{2+} by α-KA-CCMNPs, and effect of initial pH on the removal of Cu^{2+} by CCMNPs (at initial Cu^{2+} concentration 200 ppm), at magnetic nanoadsorbent dose 5 g/L, contact time 3 h, agitation speed 100 rpm, temperature $22 \pm 2\,^{\circ}C$.

3.2. Adsorption studies

3.2.1. Effect of pH and initial concentration on adsorption

The pH of the aqueous solution is an important operational parameter in the adsorption process, because it affects the speciation of copper, the surface charge, concentration of the counter ions on the functional groups of the adsorbent, and the degree of ionization of the adsorbate during reaction [34]. Fig. 6 illustrates the effect of pH and initial ion concentration on the removal efficiency of α-KA-CCMNPs and CCMNPs. For the CCMNPs, the results indicate that the maximum uptake of Cu^{2+} occurs at pH 4.0, which is similar to the previous literature [35], while the maximum uptake of Cu^{2+} occurs at pH 6.0 for α-KA-CCMNPs as shown in Fig. 6. Meanwhile, the adsorption capacity of Cu^{2+} by α-KA-CCMNPs was much greater than that by CCMNPs. For α-KA-CCMNPs, from Fig. 6, it is evident that the adsorption capacity of Cu^{2+} increases sharply as the pH increasing from 2.0–4.0 and then increases slowly at pH in 4.0–6.0. At pH in 7.0–8.0, the adsorption capacity of Cu^{2+} decreases remarkably with increasing pH. Similar trend was observed with the adsorption of copper from aqueous solution by chitosan corsslinked with a metal complexing agent [36]. This phenomenon may relate to pH_{ZPC} and the surface charge of the particles. Beyond pH 8.0, precipitate formation was observed in Cu^{2+} solution, and therefore the tests were terminated at this pH level. Consequently, Cu^{2+} adsorption shows maximum removal efficiency at the pH of 6.0.

This sorption behavior can be explained on the basis of surface change and proton-competitive sorption. The surface charge on the adsorbents is dependent on pH and provides a better understanding of the type of bond formed between Cu^{2+} and the surface. In this study the surface charge of α-KA-CCMNPs was studied by determining the point of zero charge (PZC) value of α-KA-CCMNPs using standard potentiometric method. And the PZC for α-KA-CCMNPs was found to 4.8. Namely, the surface charge is zero at the pH of 4.8. Thereby, when pH values are below the isoelectric point, the overall surface charge on the α-KA-CCMNPs become positive, which will inhibit the approach of positively charged metal ions [35]. And then, as the pH is lowered, an enhancement of positive potential in metal removal results in the increase in competition between protons and metal cations for the same functional groups and the increase in positive surface charge, as well as

results in a higher electrostatic repulsion between the surface and the metal ions. Thus, at lower pH values, the adsorption capacity of Cu^{2+} decreases with decreasing pH. When pH values are above the isoelectric point, there is a net negative charge on the surface, and the active group such as carboxyl and hydroxyl are free so as to promote interaction with the metal cations [37]. Therefore, the metal uptake increases with the increase in pH. Namely, at higher pH values, the surface of α-KA-CCMNPs has more negative charges which results in higher attraction of Cu^{2+} ions. Jha et al. [38] reported at a PZC value of 8.5 for chitosan flake. However, Udaybhaskar et al. [39] reported a PZC value in the range of 6.2–6.8 for pure chitosan. The PZC value of 4.8 and the behavior of surface charge of the α-KA-CCMNPs could have been due to the modification of chitosan after coated on γ-Fe_2O_3.

Moreover, the sorption behavior also can be explained by the hydrolysis of copper salt. The species formed by hydrolysis of copper salt are discussed by Chu and Hashim [40], and Baes and Mesmer [41]. As they explained, the main hydrolyzed copper species in the pH range of 3–6 appear to be Cu^{2+} (unhydrolyzed species), $Cu(OH)^{+}$, and $Cu(OH)_2^{0-}$. Among them Cu^{2+} is the predominant species in the solution within this pH range. In addition, carboxyl groups in α-KA-CCMNPs are considered as the main active site for adsorption of metals ions. In the pH range of 3.0–6.0, both Cu^{2+} and H^{+} ions are present. However, Cu^{2+} is able to compete better for the active sites [42]. As the pH gradually increases, the H^{+} ions decrease and Cu^{2+} ions become more available for chelation with the active groups in the α-KA-CCMNPs. Therefore, the removal efficiency of Cu^{2+} increases with the increase in the pH range of 3.0–6.0. Subsequently, when the pH value is too higher, the $Cu(OH)_2^{0-}$ are predominant and the copper hydrogen is formed. This phenomenon results in reducing the adsorption capacity of Cu^{2+} ions. Therefore, the optimum pH value for the adsorption of Cu^{2+} onto α-KA-CCMNPs is 6.0. It is worth to point out that the rest experiments in this study were all conducted at solution pH 6.

Furthermore, as shown in Fig. 6a, the similitude of the shape of curves at each initial metal ion concentration indicates that the percentage removal of Cu^{2+} decreases with the increase in the initial Cu^{2+} ion concentration. This is expected due to the fact that for a fixed adsorbent dosage, the total available adsorption sites are limited, thus leading to a decrease, corresponding to an increased initial adsorbate concentration, in percentage removal of the adsorbate.

Moreover, the TEM patterns of α-KA-CCMNPs (not shown) under the different pH are similar to Fig. 1b, which indicates there are no rodlike and rhombohedral shape of γ-Fe_2O_3 existed. This shows that the magnetic nanoparticles are not released from the α-KA-CCMNPs and the magnetic properties of α-KA-CCMNPs are preserved in the range of pH used.

3.2.2. Effect of adsorbent dose on adsorption

Since an optimum adsorbent dose is essentially required to maximize the interactions between metal ions and adsorption sites of adsorbent in the solution, the effect of adsorbent dose on Cu^{2+} ions adsorption was investigated in this part. From Fig. 7, the increase in the dose of the adsorbents increases Cu^{2+} removal efficiency at lower α-KA-CCMNPs concentrations of 0–7 g/L, whereas further increase in α-KA-CCMNPs concentrations displays a decreasing trend. Namely, the percentage removal increases as the adsorbent doses increases, but further increase in concentrations results in a decrease in removal efficiency. These observations suggest that at lower adsorbent concentrations the increase in α-KA-CCMNPs doses provides more binding sites for metal ions adsorption. However, because the increase in α-KA-CCMNPs doses and no change of the agitation speed may lead to some aggregation appeared in the system, less binding sites for metal ions are available at higher dose of α-KA-CCMNPs. Therefore, the maximum metal

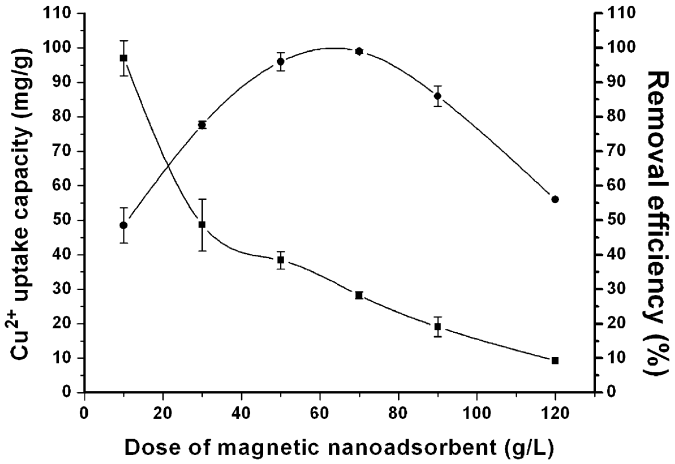

Fig. 7. Effect of magnetic nanoadsorbent dose on the removal of Cu^{2+} at initial Cu^{2+} concentration 200 ppm, contact time 3 h, initial pH 6.0, agitation speed 100 rpm, temperature 22 ± 2 °C (●, removal efficiency, %; ■, uptake capacity, mg/g).

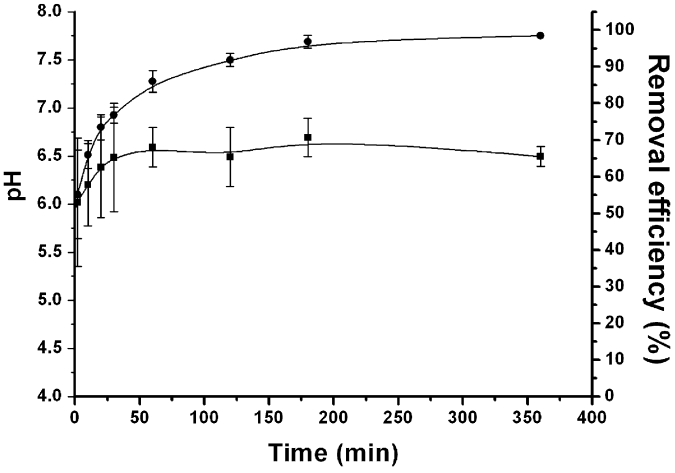

Fig. 8. Effect of contact time on the removal of Cu^{2+} by α-KA-CCMNPs at initial Cu^{2+} concentration 200 ppm, magnetic nanoadsorbent dose 5 g/L, initial pH 6.0, agitation speed 100 rpm, temperature 22 ± 2 °C (●, removal efficiency, %; ■, pH).

removal efficiency is 89.75% at 7 g/L dose of α-KA-CCMNPs. Furthermore, as shown in Fig. 7, the amount of metal ion adsorbed per unit weight of adsorbents (q) decreases with the increase in α-KA-CCMNPs doses. This is due to the fact that at higher adsorbent dose the solution ion concentration drops to a lower value, and the system reaches equilibrium at lower values of 'q' indicating the adsorption sites remain unsaturated. Therefore, from the above discussion, the adsorption capacity of Cu^{2+} ions by α-KA-CCMNPs is at optimum in the α-KA-CCMNPs concentration of 5 g/L.

3.2.3. Effect of contact time

Equilibrium time is another important operational parameter for an economical wastewater treatment process. Fig. 8 depicts the effect of contact time on the removal efficiency of Cu^{2+} by α-KA-CCMNPs. A two-stage behavior is observed. It is observed from the results that the uptake of Cu^{2+} is initially quite high, and slows down with the lapse of time leading gradually to an equilibrium condition. It also shows that a major fraction of Cu^{2+} is adsorbed onto α-KA-CCMNPs during the first 180 min, while only a very small part of the additional adsorption occurs during the following contact time. This clearly suggests that the adsorption of metal cations on the surface of α-KA-CCMNPs could take place in a single step and without any complexity. Thus, it is possible that during the initial stage of the process, the surface coverage is low, and

adsorptive ions occupy active surface sites rapidly in a random manner. As a result, the rate of uptake is higher. As time lapses the surface coverage increases, the rate of uptake becomes slower in latter stages, and ultimately an almost plateau region is attained when surface become saturate. It has to be noted that, from Fig. 8, the removal efficiency reached 50% within 2 min, which is much faster than that of other reports [43–45], and the equilibrium is attained around 60 min. In order to get the maximum uptake, the contact time was determined to be 3 h during the batch studies.

Furthermore, a rather fast uptake of Cu^{2+} ions and a small increase of pH values from 6.0 to 6.5 simultaneously occur within the first 30 min. It is known that the adsorption of Cu^{2+} ions should result in a release of H^+ ion. This should normally reduce the pH of the solution. However, Kaminski and Modrzejewska [46] noted that the exchange of released H^+ ions occurs between the surface of the bead and solution resulting in the increase of pH of the solution. Thus, the rather fast uptake of Cu^{2+} ions results in the increase in pH.

3.3. Adsorption isotherm

Adsorption isotherms are important for the description of how adsorbates will interact with an adsorbent, and are critical in optimizing the use of adsorbents. Adsorption equilibrium studies estimate the capacity of the adsorbent. It is described by adsorption isotherms characterized by certain constants whose values express the surface properties and affinity of the adsorbent [47].

The Langmuir and Freundlich isotherm model are often used to describe equilibrium sorption isotherms. The Langmuir model originally developed for adsorption of gases onto solids assumes that adsorption occurs in a monolayer or that adsorption may only occur at a fixed number of localized sites on the surface with all adsorption sites identical and energetically equivalent. Therefore, the Langmuir equation is based on the assumptions of a structurally homogeneous adsorbent, and is described by the following equation:

$$\frac{C_e}{q_e} = \frac{C_e}{q_0} + \frac{1}{q_0 b}, \tag{3}$$

where q_e is the amount of Cu^{2+} adsorbed per unit weight of adsorbents at specified equilibrium (mg/g), C_e the equilibrium concentration in the solution (mg/L), q_0 the maximum adsorption at monolayer coverage (mg/g), and b is the Langmuir constant related to the affinity of binding sites (L/mg), and is a measure of the energy of adsorption. The essential characteristics of Langmuir isotherm model can be explained in terms of a dimensionless constant separation factor or equilibrium parameter R_L [48], which is defined by

$$R_L = \frac{1}{1 + bC_0}, \tag{4}$$

where b is Langmuir constant (L/mg), and C_0 is the initial concentration (mg/L). It has been shown using mathematical calculations that parameter R_L indicates the shape of the isotherms. The R_L value classified as $R_L > 1$, $0 < R_L < 1$ and $R_L = 0$ suggest that adsorption is unfavorable, favorable and irreversible, respectively [48].

The maximum adsorption (q_0) and the values of Langmuir constants for the Cu^{2+} adsorption calculated from the slope and the intercept of the linear plot are shown in Table 1.

Alternatively, the Freundlich equation [49] is an empirical equation based on adsorption on a heterogeneous surface. The equation is commonly represented by

$$\log q_e = \log k + \frac{1}{n} \log C_e, \tag{5}$$

Table 1
Langmuir and Freundlich constants for the adsorption of Cu^{2+} by two adsorbents.

Adsorbent	Langmuir constants				Freundlich constants		
	b (L/mg)	q_0 (mg/g)	R^2	R_L[a]	k	$1/n$	R^2
α-KA-CCMNPs	0.0493	96.15	0.9955	0.0921	16.406	0.3018	0.6573
CCMNPs	0.0174	60.606	0.8915	0.2231	10.772	0.2452	0.8524

[a] R_L for C_0 of 200 ppm is calculated by Eq. (4).

where q_e and C_e have the same definitions as in Eq. (3), k is a Freundlich constant representing the adsorption capacity, and n is a constant depicting the adsorption intensity (dimensionless). The values of Freundlich constants n and k for the adsorption of Cu^{2+} calculated from the slope and the intercept of the linear plot are shown in Table 1.

From Table 1, the value of the correlation coefficient (R^2) for the Langmuir equation (0.9955) is much higher than that for the Freundlich equation (0.6573). Thus, the adsorption data fit well with the Langmuir isotherm. The adsorption data of Cu^{2+} according with Langmuir isotherm illustrate that the binding energy on the whole surface of α-KA-CCMNPs is uniform. In other words, the whole surface has identical adsorption activity. The adsorption data of Cu^{2+} according with Langmuir isotherm also show that the adsorbed metal ions do not interact or compete with each other, and they are adsorbed by forming a monolayer. This phenomenon, at the same time, indicates that chemosorption is the principal removal mechanism in adsorption process. Moreover, the maximum adsorption capacity of α-KA-CCMNPs, determined to be 96.15 mg/g, is considerably higher than that of other reported magnetic adsorbents, such as pure γ-Fe_2O_3 (19.4 mg/g) [14], δ-FeOOH-coated γ-Fe_2O_3 (25.8 mg/g) [14], chitosan-bound Fe_3O_4 nanoparticles (21.5 mg/g) [17], and carboxymethyl chitosan–Fe_3O_4 nanoparticles (20.4 mg/g) [50]. Meanwhile, because the q_0 value is higher than that of the experimental q_{eq}, it may be also suggested that adsorption takes place as monolayer phenomena; in other words, α-KA-CCMNPs are fully covered by Cu^{2+} ions.

Adsorption isotherms for CCMNPs are also investigated. The Langmuir and Freundlich constants for the adsorption of Cu^{2+} calculated from the slope and the intercept of the linear plot and the correlation coefficients (R^2) are also shown in Table 1. And the correlation coefficients (R^2) of CCMNPs indicate that the adsorption data for the Cu^{2+} removal do not fit well with either the Langmuir or the Freundlich isotherm due to the low correlation coefficients.

The equilibrium adsorptions of Cu^{2+} by α-KA-CCMNPs and CCMNPs as a function of the initial Cu^{2+} ion concentration are shown in Fig. 9. From Fig. 9, it is seen that the adsorption capacity increases with the increasing of initial Cu^{2+} ion concentrations for both α-KA-CCMNPs and CCMNPs until equilibrium was attained. Similar behavior was reported by Anjana et al. [51], Jong et al. [52] and Li et al. [53]. However, the increase in adsorption capacity for α-KA-CCMNPs is always much greater than that for CCMNPs. Moreover, the correlation coefficient (R^2) of Langmuir equation for α-KA-CCMNPs (0.9955) is higher than that of Langmuir equation for pure CCMNPs (0.8915), and that of Freundlich equation for pure CCMNPs (0.8524). These findings indicate that the α-KA-CCMNPs are better adsorbents, and the surface-modified can enhance the Cu^{2+} adsorption capacity. By calculation, R_L is often between 0 and 1, regardless of the initial concentration of Cu^{2+} (see Table 1). This result indicates that the adsorption of Cu^{2+} by α-KA-CCMNPs is favorable.

3.4. Regeneration studies

Since Cu^{2+} adsorption is a reversible process, the regeneration or activation of the adsorbent can be considered. The primary

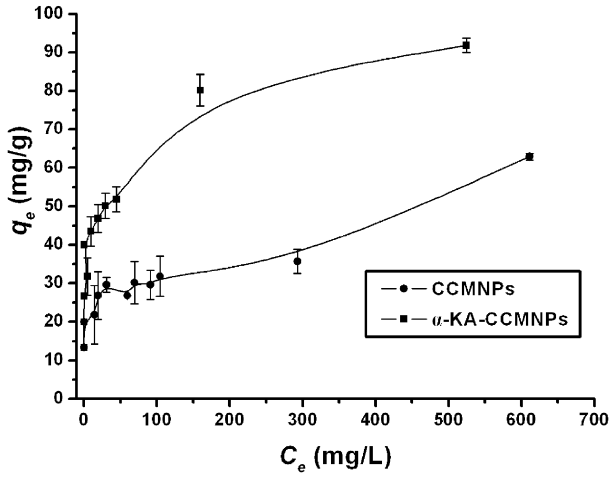

Fig. 9. The relationship of C_e and adsorption capacities for the α-KA-CCMNPs and the CCMNPs.

Table 2
Eluents for desorption and the desorption efficiency of Cu^{2+}.

Eluents	Desorption efficiency (%)
100 mmol/L Na_2EDTA	91.5
25 mmol/L Na_2EDTA	61.5
100 mmol/L HCl	26.5
25 mmol/L HCl	24
100 mmol/L citric acid	24
25 mmol/L citric acid	21.5
100 mmol/L acetic acid	49
25 mmol/L acetic acid	26.5

objective of regeneration is to restore the adsorption capacity of exhausted adsorbents while the secondary objective is to recover valuable metals present in the adsorbed phase, if any. Four kinds of chemicals (see Table 2) were chosen as eluents. Among these stripping solution, a 100 mmol/L Na_2EDTA reveals the highest desorption efficiency compared to another concentration of Na_2EDTA and other eluents or the same concentration of other eluents. The quantitative desorption efficiency of 100 mmol/L Na_2EDTA is up to 90%. The desorption efficiency of Cu-α-KA-CCMNPs using the above stripping solutions was illustrated in Table 2. Moreover, the sample after adsorption was examined by XRD technique. And the result from the XRD pattern shows that the main peaks of γ-Fe_2O_3 in Cu-α-KA-CCMNPs (Fig. 3c) are similar to those in α-KA-CCMNPs before adsorption (Fig. 3b), except for the peaks of Cu which is affirmed by Cu standard data. Meanwhile, the XRD result of α-KA-CCMNPs collected after desorption (Fig. 3d) is not changed relative to that of fresh ones (Fig. 3b)—there is no any new crystalline phases generated. Similarly, the sample after desorption was also examined by FTIR technique. And the result of the FTIR spectrum shows that the main peaks of the function groups on the surface of α-KA-CCMNPs after desorption (Fig. 2e) are similar to those on the surface of α-KA-CCMNPs before adsorption (Fig. 2d). The α-KA-CCMNPs are thus verified to be effective and stable in the adsorption and desorption process. After the optimization of the stripping solutions, the regeneration cycles were repeated for 7 cycles using 50 mg of α-KA-CCMNPs and 10 ml of 200 ppm $CuSO_4$ solution for the adsorption process, and the desorption process was carried out with 10 ml of 100 mmol/L Na_2EDTA. The Cu^{2+} adsorption and desorption capacity of α-KA-CCMNPs undergoing seven cycles is presented in Fig. 10. It is observed that Cu^{2+} adsorption capacity of α-KA-CCMNPs remains almost constant for the seven cycles, which indicates that there are no irreversible sites on the surface of α-KA-CCMNPs.

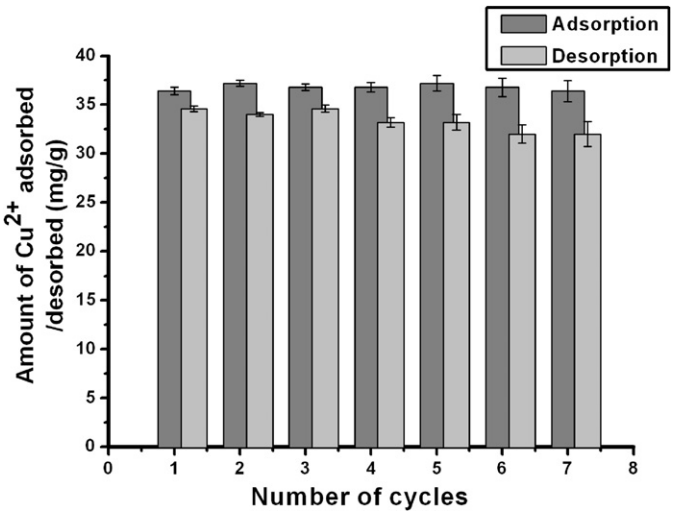

Fig. 10. Adsorption and desorption cycles: adsorption-initial Cu^{2+} concentration 200 ppm; magnetic nanoadsorbent dose 5 g/L; contact time 3 h; initial pH 6.0; agitation speed 100 rpm; temperature 22 ± 2 °C; desorption-sample volume, 10 ml of 0.1 M Na_2EDTA; contact time 0.5 h; agitation speed 100 rpm.

3.5. Cost estimation

The α-KA, as a kind of modification reagent, is a harmless and environmental-friendly biologic reagent, while the chemical modification reagents are general toxic to the human, animal and enzyme, and the cost of them is expensive. The cost of the α-KA-CCMNPs arises mainly from the α-KA which price is about US$ 380 kg^{-1} depending on the preparation procedure. However, the costs of the chitosan flakes cross-linked with glutaraldehyde and chitosan-coated polyvinyl chloride beads are US$ 15,700 kg^{-1} [54] and US$ 3254 kg^{-1} [35], respectively. Moreover, the data presented indicate that α-KA-CCMNPs can work well for the metal ions removal from aqueous solution. The removal efficiency of α-KA-CCMNPs reached 50% within 2 min, and the adsorption equilibrium of α-KA-CCMNPs was attained just about 60 min. But the equilibrium time of the chitosan flakes cross-linked with glutaraldehyde is sixteen times than that of α-KA-CCMNPs. And the equilibrium time of the chitosan-coated polyvinyl chloride beads is 200 min, which is almost three times than that of α-KA-CCMNPs. Namely, one of the obvious advantages of α-KA-CCMNPs is its fast adsorbing speed, and therefore requiring much less process cost. Meanwhile, the maximum uptake of the α-KA-CCMNPs is 96.15 mg/g, while that of the chitosan flakes cross-linked with glutaraldehyde or chitosan-coated polyvinyl chloride beads is 85.5 or 87.9 mg/g, respectively. In other words, the maximum uptake of α-KA-CCMNPs is also greater than that of either of these two adsorbents. Considering the above facts, the α-KA-CCMNPs can be considered as an economical alternative for the commercially available adsorbents in removal of Cu^{2+} from aqueous solution.

4. Summary

In this study, a novel magnetic nanoadsorbent comprising CCMNPs modified with α-KA was successfully prepared for effectively removing Cu^{2+} from aqueous solution. Physical characterization from VSM measurement shows that the superparamagnetic properties of α-KA-CCMNPs do not decrease markedly after coating, modification and Cu^{2+} adsorption processes. And the saturation magnetization of α-KA-CCMNPs after coating, modification and Cu^{2+} adsorption processes was much higher than other magnetic adsorbents in the reported references [30–33]. These large saturation magnetization and superparamagnetic properties made α-KA-CCMNPs very susceptible to the external magnetic field, and

possibly reusable without aggregation after removing the external magnetic field. Batch adsorption tests determined the effectiveness of α-KA-CCMNPs as an alternative sorptive material. Adsorption of Cu^{2+} reaches equilibrium within 60 min and 50% of Cu^{2+} being adsorbed at 2 min. Adsorption equilibrium studies show that Cu^{2+} adsorption data follow the Langmuir model. The maximum adsorption capacity of α-KA-CCMNPs, determined to be 96.15 mg/g, is considerably higher than that of other reported magnetic adsorbents [14,17,50]. Compared with CCMNPs, the removal efficiency of Cu^{2+}, adsorbed by α-KA-CCMNPs, was enhanced significantly. The regeneration tests, XRD and FTIR investigation illustrates the high stability and recovery capacities of α-KA-CCMNPs. Furthermore, no release of γ-Fe_2O_3 was observed during the experiments. Consequently, the experimental results and cost estimation suggest that, as a kind of potential adsorbent, the α-KA-CCMNPs can remove heavy metals from wastewater efficiently using the technology of magnetic separation, and that this process can be competitive with the conventional technologies. Finally, the studies are still continuing, and more detailed results will appear in a forthcoming paper.

Acknowledgments

This work was supported by Program for Changjiang Scholars and Innovative Research Team in University (IRT0526) and the National Natural Science Foundation of China (50773009). This work was also supported in part by UK-CHINA Joint Laboratory for Therapeutic Textiles based in Donghua University and Biomedical Textile Materials “111 Project,” Ministry of Education of P.R. China (No. B 07024).

References

[1] S.S. Banerjee, D.H. Chen, J. Hazard. Mater. 147 (2007) 792.
[2] A. Kortenkamp, M. Casadevall, S.P. Faux, A. Jenner, R.O.J. Shayer, N. Woodbrige, P. O'Brien, Arch. Biochem. Biophys. 329 (2) (1996) 199.
[3] B. Murphy, B. Hathaway, Coord. Chem. Rev. 243 (2003) 237.
[4] S. Rengaraj, Y. Kim, C.K. Joo, J. Yi, J. Colloid Interface Sci. 273 (2004) 14.
[5] C.A. Flemming, J.T. Trevors, Water Air Soil Pollut. 44 (1989) 143.
[6] K. Kadirvelu, C. Namasivayam, Adv. Environ. Res. 7 (2003) 471.
[7] N. Chiron, R. Guilet, E. Deydier, Water Res. 37 (2003) 3079.
[8] J.G. Dean, F.L. Bosqui, K.L. Lannouette, Environ. Sci. Technol. 6 (1997) 518.
[9] G. Dönmez, Z. Aksu, Process Biochem. 35 (1999) 135.
[10] B. Volesky, Z.R. Holan, Biotechnol. Prog. 11 (1995) 235.
[11] C.Z. Huang, B. Hu, Spectrochim. Acta B 63 (2008) 437.
[12] V. Rocher, J.M. Siaugue, V. Cabuil, A. Bee, Water Res. 42 (2008) 1290.
[13] A. Henglein, Chem. Rev. 89 (1989) 1861.
[14] J. Hu, M.C.I. Lo, G.H. Chen, Sep. Purif. Technol. 58 (2007) 76.
[15] R.L. Kochen, J.D. Navratil, Rosenblatt & Redano P.C., Satellite or other remote site system for well control and operation, US Patent 5955666, 1997.
[16] A.F. Ngomsik, A. Bee, J.M. Siaugue, V. Cabuil, G. Cote, Water Res. 40 (2006) 1848.
[17] Y.C. Chang, D.H. Chen, J. Colloid Interface Sci. 283 (2005) 446.
[18] M. Kaminski, Sep. Sci. Technol. 32 (1997) 115.
[19] J.H.P. Watson, D.C. Ellwood, R.G. Lidzey, In: Proc. Int. Conf. Radioact. Waste Manage. Environ. Remediat. vol. 2, 2003, p. 1203.
[20] Y.S. Kang, S. Rishud, J.F. Rabolt, P. Stroeve, Chem. Mater. 8 (1996) 2209.
[21] P. Ding, K.L. Huang, G.Y. Li, W.W. Zeng, J. Hazard. Mater. 146 (2007) 58.
[22] Z.Q. Ren, W.D. Zhang, Y.M. Liu, Y. Dai, C.H. Cui, Chem. Eng. Sci. 62 (2007) 6090.
[23] C.K. Liu, R.B. Bai, Q.S. Ly, Water Res. 42 (2008) 1511.
[24] C. Quintelas, B. Fernandes, J. Castro, H. Figueiredo, T. Tavares, J. Hazard. Mater. 153 (2008) 799.
[25] Z.Y. He, H.L. Nie, C.B. White, L.M. Zhu, Y.T. Zhou, Y. Zheng, Bioresour. Technol. 99 (2008) 7954.
[26] Z.H. Jing, S.H. Wu, Mater. Lett. 58 (2004) 3637.
[27] S.H. Xu, W. Shangguan, J. Yuan, M.X. Chen, J.W. Shi, Appl. Catal. B 71 (2007) 177.
[28] J. Lee, T. Isobe, M. Senna, J. Colloid Interface Sci. 177 (1996) 490.
[29] W. Yantasee, C.L. Warner, T. Sangvanich, R.S. Addleman, T.G. Carter, R.J. Wiacek, G.E. Fryxell, C. Timchalk, M.G. Warner, Environ. Sci. Technol. 41 (2007) 5114.
[30] Z.Y. Ma, Y.P. Guan, H.Z. Liu, J. Polym. Sci. Part. A Polym. Chem. 43 (2005) 3433.
[31] Z.Y. Ma, Y.P. Guan, X.Q. Liu, H.Z. Liu, Chin. J. Chem. Eng. 13 (2005) 239.
[32] Y. Lee, J. Rho, B. Jung, J. Appl. Polym. Sci. 89 (2003) 2058.
[33] X.Q. Liu, Y.P. Guan, R. Shen, H.Z. Liu, J. Chromatogr. B 822 (2005) 91.
[34] S.M. Nomanbhay, K. Palanisamy, Electron. J. Biotechnol. 8 (2005) 43.
[35] S.R. Popuri, Y. Vijaya, V.M. Boddu, K. Abburi, Bioresour. Technol. 100 (2009) 194.
[36] H.L. Vasconcelos, T.P. Camargo, N.S. Gonçalves, A. Neves, M.C.M. Laranjeira, V.T. Fávere, React. Funct. Polym. 68 (2008) 572.
[37] S.Y. Quek, D.A.J. Wase, C.F. Forster, Water SA. 24 (1998) 251.
[38] I.N. Jha, L. Iyenger, A.V.S.P. Rao, J. Environ. Eng. 114 (4) (1998) 964.
[39] P. Udaybhaskar, L. Iyenger, R.J. Prabhakar, J. Appl. Polym. Sci. 39 (1990) 739.
[40] K.H. Chu, A.A. Hashim, J. Chem. Technol. Biotechnol. 75 (2000) 1054.
[41] C.F. Baes Jr., R.E. Mesmer, The Hydrolysis of Cations, Wiley, 1967.
[42] S. Hasan, T.K. Ghosh, D.S. Viswanath, V.M. Boddu, J. Hazard. Mater. 152 (2008) 826.
[43] Y.M. Ren, X.Z. Wei, M.L. Zhang, J. Hazard. Mater. 158 (2008) 14.
[44] P.M. Pimentel, M.A.F. Melo, D.M.A. Melo, A.L.C. Assuncao, D.M. Henrique, C.N. Silva Jr., G. Gonzalez, Fuel Process. Technol. 89 (2008) 62.
[45] W.H. Zou, R.P. Han, Z.Z. Chen, J.H. Zhang, J. Shi, Colloids Surf. A 279 (2006) 238.
[46] W. Kaminski, Z. Modrzejewska, Sep. Sci. Technol. 32 (16) (1997) 2659.
[47] A.E. Silkaily, A.E. Nemr, A. Khaled, O. Abdelwehab, J. Hazard. Mater. 148 (2007) 216.
[48] Y. Zhai, X. Wei, G. Zeng, D. Zhang, K. Chu, Sep. Purif. Technol. 38 (2004) 191.
[49] H. Freundlich, Z. Phys. Chem. 57A (1907) 385.
[50] L.M. Zhou, Y.P. Wang, Z.R. Liu, Q.W. Huang, Acta Phys. Chim. Sin. 22 (11) (2006) 1342.
[51] K. Anjana, A. Kaushik, B. Kiran, R. Nisha, J. Hazard. Mater. 148 (2007) 383.
[52] T. Jong, D.L. Parry, J. Colloid Interface Sci. 275 (2004) 61.
[53] N. Li, R. Bai, Sep. Purif. Technol. 42 (2005) 237.
[54] N. Sankararamakrishnan, A.K. Sharma, R. Sanghi, J. Hazard. Mater. 148 (2007) 353.